Journal of Polymer Science and Engineering 2024, 7(1), 4576.
https://doi.org/10.24294/jpse.v7i1.4576

Article

An analysis of temperature control for electromagnetic induction heating of CFRP based on sparrow search algorithm

Ning Yang[1], Tianyu Fu[2,*]

[1] School of Computer and Network Engineering, Shanxi Datong University, Datong 037000, China
[2] Intelligent Equipment College, Changzhou Information Vocational and Technical College, Changzhou 213000, China
*** Corresponding author:** Tianyu Fu, 827263230@qq.com

CITATION

Yang N, Fu T. An analysis of temperature control for electromagnetic induction heating of CFRP based on sparrow search algorithm. Journal of Polymer Science and Engineering. 2024; 7(1): 4576. https://doi.org/10.24294/jpse.v7i1.4576

ARTICLE INFO

Received: 6 February 2024
Accepted: 26 March 2024
Available online: 13 May 2024

Abstract: Accurate temperature control during the induction heating process of carbon fiber reinforced polymer (CFRP) is crucial for the curing effect of the material. This paper first builds a finite element model of induction heating, which combines the actual fiber structure and resin matrix, and systematically analyzes the heating mechanism and temperature field distribution of CFRP during the heating process. Based on the temperature distribution and variation observed in the material heating process, a PID control method optimized by the sparrow search algorithm is proposed, which effectively reduces the temperature overshoot and improves the response speed. The experiment verifies the effectiveness of the algorithm in controlling the temperature of the CFRP plate during the induction heating process. This study provides an effective control strategy and research method to improve the accuracy of temperature control in the induction heating process of CFRP, which helps to improve the results in this field.

Keywords: carbon fiber; temperature control; temperature field distribution

1. Introduction

The superior physical and chemical properties of CFRP make it increasingly widely used in daily life, especially in the fields of aerospace, automobiles, and energy, where the application scope of CFRP is constantly expanding and its consumption is increasing year by year. This puts forward higher standards for the heating rate, energy utilization, and pollutant emission of CFRP in the curing process. For this purpose, scholars have proposed many innovative curing and molding methods, such as infrared thermal radiation, resistance heating, ultraviolet light, induction heating, etc. Among them, induction heating technology has many advantages, such as high efficiency, energy savings, a small footprint, non-contact, etc. Combining it with the curing and molding of CFRP can significantly improve the heating rate of the material, reduce manufacturing costs, and reduce the intrusion of external impurities. However, the arrangement of carbon fibers inside the material directly affects the heating effect and the distribution of the temperature field during the heating process, and the distribution of the temperature field directly affects the molding quality of the composite material. Therefore, it is necessary to explore the spatiotemporal variation of the temperature field generated by CFRP with different fiber arrangement modes in the induction heating process.

The application of induction heating technology in CFRP curing and molding is increasing, which has attracted the high attention of scholars in the industry, and they have conducted in-depth research on the heating principle and temperature distribution of CFRP in the induction heating process. Fink et al. [1] discussed that the condition

for forming an eddy current in CFRP during induction heating is that there is an effective closed circuit between the fibers. For this purpose, carbon fiber bundles need to be cross-woven in other ways to form the laminated structure of CFRP. Yarlagadda et al. [2] analyzed the three overlapping contact modes of fiber bundles during weaving, which correspond to three heating modes of resistance heating, capacitance heating, and resistive-capacitive heating, respectively, affecting the heat generation and heating rate at the nodes. Kim et al. [3]. studied the method to determine the dominant heating mechanism of carbon fiber induction heating under different weaving/overlapping modes, and established a numerical analysis model of CFRP induction heating including three heating mechanisms. Lundström et al. [4]. established a finite element simulation model of CFRP induction heating, and studied the influence of carbon fiber volume fraction, laying mode, and fiber orientation on the temperature field distribution of CFRP induction heating.

When induction heating CFRP, the heating process, temperature regulation speed, and temperature value accuracy of the temperature field directly determine the molding quality of CFRP, so the control algorithm is very important for the production of induction heating CFRP. The performance of the controller is affected by the parameter adjustments [5,6]. In order to find the suitable controller parameter set, there are many methods proposed, such as the Ziegler-Nichols method [7], the ant colony optimization algorithm [8,9], and the neural network method [10]. However, the model of the induction heating system changes with the environment, induction coil, and workpiece. Therefore, the neural network lacks a pre-trained data set. Some studies [5,11,12] show that a fuzzy PID controller that combines the structure of a PID controller and the expert knowledge of FIS, has excellent control performance. Soyguder et al. [13] designed an adaptive fuzzy PID controller, which adjusts the PID parameters online according to the temperature error and error change rate of the HVAC system, and achieves the minimum setting time and zero steady-state error. Chang et al. [14] deeply analyzed all the quantization factors and developed a self-tuning module that used finite element analysis to simulate the control ability of a self-tuning fuzzy logic controller and conducted experiments on the induction heating system, verifying the effectiveness of the method. Chowdhury et al. [15] proposed a fuzzy self-tuning PID controller for a preheating recovery system, tested the set point tracking and disturbance suppression ability in steady-state and transient heat cases, and found that the fuzzy self-tuning PID controller greatly reduced the calculation time and significantly improved the control performance. Wang et al. [16] proposed a temperature control method of induction heating system based on a variable domain fuzzy controller, and the simulation results showed the effectiveness and superiority of the temperature control system. These studies prove the effectiveness of fuzzy PID in temperature control systems, but for induction heating CFRP, which is a fast heating system, the accurate mathematical model and robustness of the temperature control system are very important.

In order to avoid falling into the local optimum and ensure control accuracy and optimization performance, this paper proposes a PID control algorithm based on sparrow search (SSA-PID) and compares SSA-PID with particle swarm optimization PID algorithm (PSO-PID) and PID control. The conclusion is that SSA-PID has a smaller overshoot and faster adjustment time than the other two algorithms.

2. CFRP induction heating principle and analysis

Alternating magnetic field generates an induced electric field $E(V/m)$ in carbon fiber structure, which can be expressed in the form of frequency as follows:

$$E = -j\omega A \tag{1}$$

In the equation, $j^2 = -1$, $\omega = 2 * \pi f(rad/s)$ is the angular frequency, and $f(Hz)$ is the magnetic field frequency.

The total current sum generated in the fiber structure consists of conduction current $J_i = \sigma E$ and displacement current $J_d = j\omega D$:

$$J_t = J_t + J_d = \sigma E + j\omega D \tag{2}$$

The eddy current in the fiber structure and the Joule heat generated by its own resistance are the heating heat sources of CFRP, where the heat source $Q_{rh,i}$ (W/m^3) can be expressed as follows:

$$Q_{rh,i} = J_t \cdot E \tag{3}$$

When the power supply is activated, the heat generated by the induced current in the fiber bundle is transferred to the surrounding fiber bundle, resin, and ambient air. The heat conduction of the fiber part can be expressed by Fourier's law of heat conduction:

$$\rho C_p \frac{\partial T}{\partial t} + \nabla \cdot (-k\nabla T) = Q \tag{4}$$

In the equation, ρ(Kg/m^3) is the density of the material, C_p(J/kg·K) is the specific heat capacity of the material, k(W/m·K) is the thermal conductivity of the material, and Q(W/m^3) is the heat emitted by the heat source.

As epoxy resin is a phase change material, it releases heat during the curing process from liquid to solid. The heat conduction equation when the phase change occurs in the resin is as follows:

$$\rho C_p \mu \cdot \nabla T + \nabla \cdot (-k\nabla T) = Q \tag{5}$$

In the equation, μ(m/s) is the flow velocity of the resin when heated.

The resin gradually releases latent heat L(J/Kg) during the process of gradually changing from the liquid phase to the solid phase during heating. Since we only consider the heat release of the material during heating, in order to make it easier to calculate, we assume that the phase change temperature of the resin occurs between $T_{pc} - \Delta T/2$ and $T_{pc} + \Delta T/2$. In the interval of phase change reaction, the material is modeled by a smooth function; θ represents the fraction of phase in the transition process, from $\theta = 0$ when the temperature is $T_{pc} - \Delta T/2$, to $\theta = 1$ when the temperature reaches $T_{pc} + \Delta T/2$. In the equation, ρ is the density of the material, and H is the specific enthalpy, which will be expressed as follows:

$$C_p = H + C_L(T) = \frac{1}{\rho}(\theta\rho_1 C_{p1} + (1-\theta)\rho_2 C_{p2}) + L\frac{\partial \alpha}{\partial T} \tag{6}$$

The latent heat distribution C_L can be expressed as follows:

$$C_L = L\frac{\partial \alpha}{\partial T} \tag{7}$$

The total heat released per unit volume during phase change is equal to the latent heat:

$$\int_{T_{pc}-\frac{\Delta T}{2}}^{T_{pc}+\frac{\Delta T}{2}} C_L(T)dT = L\int_{T_{pc}-\frac{\Delta T}{2}}^{T_{pc}+\frac{\Delta T}{2}} \frac{d\alpha}{dT}dT = L \tag{8}$$

In the induction heating process, when the temperature of the object is higher than the external environment, the heated object exchanges heat with the surrounding environment after heating, and the exchange with the air is the most important, so the convective heat flux of the air needs to be considered:

$$-k\nabla T = h(T_{amb} - T) \tag{9}$$

In the equation, h(W/m^{2}K) is the heat transfer coefficient determined by the boundary type and surface properties, T_{amb} is the external air temperature, and T is the surface temperature of the heated material.

When the temperature gradually rises, the thermal radiation generated by the material needs to be considered, and the diffuse surface uniformly releases radiation intensity in all directions. The surface radiation intensity of the material is:

$$-k\nabla T = \varepsilon\gamma(T_{amb}^4 - T^4) \tag{10}$$

In the equation, ε is the emissivity of the material surface, and γ is the Boltzmann constant.

This study uses COMSOL as the simulation platform and establishes a finite element analysis model with the plain weave structure of CFRP as the geometric model, as shown in **Figure 1**. The size of CFRP in the model is 60 mm × 60 mm × 5 mm, the induction coil size is φ30 × 20 mm, the number of turns is 50, the current size is 16A, the frequency size is 13 kHz, the external environment temperature is 20 ℃, and the distance between the coil and the carbon fiber surface is 2.5 mm. The parameters assigned to each material in the geometric model are shown in **Table 1**, and the parameters are obtained from the CFRP manufacturers and the COMSOL material library.

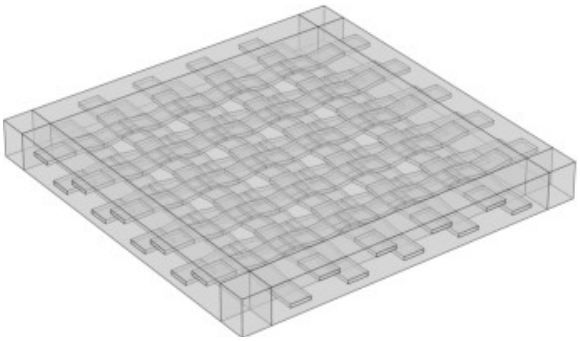

Figure 1. Finite element analysis model of plain weave structure CFRP.

Table 1. Simulation parameters.

	Air	Carbon fiber bundle	Resin	Coils
Thermal Conductivity (W/(m·K))	N/A	30	0.2	N/A
Heat Capacity (J/(kg·K))	N/A	1000	1000	N/A
Density (kg/m^3)	N/A	1500	1200	8960
Electrical Conductivity (S/m)	0	6.4 × E^4	1 × E^{-2}	6 × E^7
Relative Permittivity	1	—	3.2	1
Relative Permeability	1	1	1	1

From the simulation results in **Figure 2**, it can be seen that when induction heating CFRP, the temperature rise of the material mainly occurs in the heat source area near the outer circle of the induction coil in the initial stage and presents a ring-shaped temperature field distribution. With the increase in heating time, the heat transfers along the fiber bundle direction, making the overall temperature of the material rise. The temperature field distribution also gradually changes from ring-shaped to cross-shaped, spreading along the X-axis and Y-axis directions. The center area of the material heats up the fastest and finally reaches the same temperature as the heat source area, and the value is the largest.

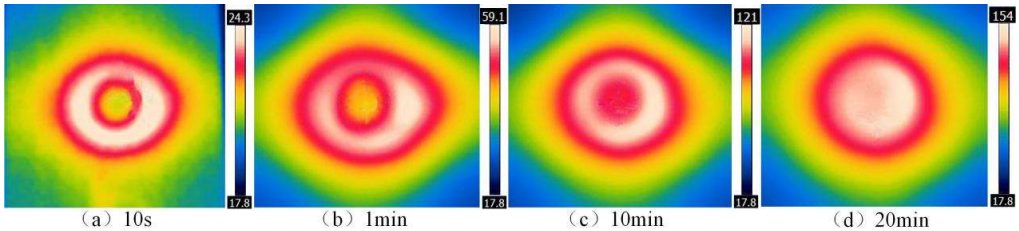

Figure 2. Change rules of temperature field of CFRP induction heating.

3. Induction heating temperature control

3.1. Sparrow search algorithm principle

In the induction heating process, the mixing mode of the resin matrix and fiber structure in carbon fiber composite material, as well as the interlayer heat conduction process, will cause a difference between the temperature value recorded by the infrared sensor and the actual internal temperature value of the material. In addition, the inherent lag of the temperature control system makes it more challenging to control the temperature of CFRP during heating. This is especially important in the curing and molding process of CFRP because a high temperature value will affect the molding quality of the material. Therefore, reducing overshoot in the material heating process is essential for improving the quality of material curing and molding. In order to realize the quantifiable optimization of control factors and improve control accuracy, this study adopts a sparrow search algorithm to optimize the PID control method. The schematic principle of the control method is shown in **Figure 3**, and the flow chart of the method is shown in **Figure 4**.

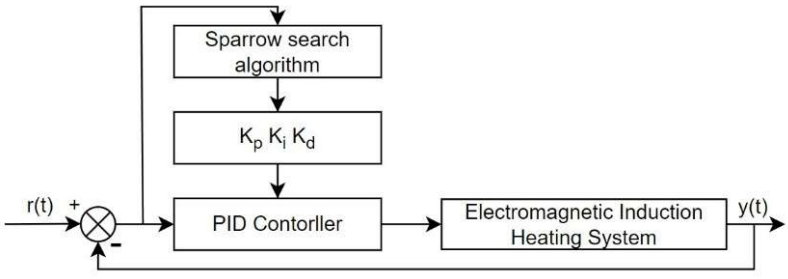

Figure 3. Schematic diagram of PID algorithm optimized by the sparrow search algorithm.

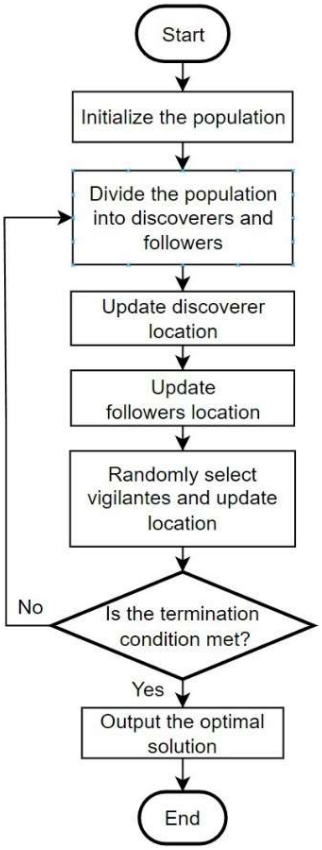

Figure 4. PID control algorithm flow chart optimized by the sparrow search algorithm.

First, calculate the current fitness value of each sparrow and store the individual and position information in the local extremum. Traverse the individual extremum, select the optimal individual information, and store it in the global extremum. In order to ensure that the parameters have good selectivity, the fitness function defined in this paper is as follows:

$$f(x) = \sum_{i=1}^{d} x_i^2 \tag{11}$$

where *x* represents the position of the sparrow, and d represents the dimension. Then, update the weight and learning factor, and modify the critical value of the crossover probability. The crossover probability here is not a fixed value but is adjusted according to the size of the population difference to avoid falling into the local optimum in the later stage of evolution. By increasing the crossover probability in the later stage, we can effectively escape from the local optimum. In addition, the equation for updating the weight is as follows (12), the equation for updating the learning factor is as follows (13 and 14), and the equation for modifying the adaptive crossover probability is as follows (15).

$$w = w_{max} - \frac{w_{max} - w_{min}}{iter_{max}} \cdot iter \tag{12}$$

$$c_1 = c_{1max} - \frac{c_{1max} - c_{1min}}{iter_{max}} \cdot iter \tag{13}$$

$$c_2 = c_{2max} - \frac{c_{2max} - c_{2min}}{iter_{max}} \cdot iter \tag{14}$$

$$p_c = 0.5 + \frac{0.5}{1 + \exp\left(-\frac{f_g - f_w}{f_g + f_w + \varepsilon}\right)} \tag{15}$$

where, w represents the inertia weight, w_{max} and w_{min} respectively represent the maximum and minimum values of the inertia weight, $iter$ represents the current iteration number, $iter_{max}$ epresents the maximum iteration number, c_1 and c_2 respectively represent the first and second learning factors, c_{1max} and c_{1min} respectively represent the initial and minimum values of the first learning factor, c_{2max} and c_{2min} respectively represent the initial and minimum values of the second learning factor, p_c represents the crossover probability, f_g and f_w respectively represent the global optimal fitness value and the global worst fitness value, ε represents a small constant, used to avoid the denominator being zero.

Then, update the speed and position of the sparrows according to Equations (16) and (17). Next, calculate the new fitness value matrix of the individuals in the population, and prepare for the subsequent genetic algorithm. If the sparrows are out of bounds, randomly generate new positions and speeds within the specified range, and replace the current positions and speeds.

$$v_{i,j}^{t+1} = w \cdot v_{i,j}^{t} + c_1 \cdot R_1 \cdot \left(x_{p,j}^{t} - x_{i,j}^{t}\right) + c_2 \cdot R_2 \cdot \left(x_{g,j}^{t} - x_{i,j}^{t}\right) \tag{16}$$

$$x_{i,j}^{t+1} = x_{i,j}^{t} + v_{i,j}^{t+1} \tag{17}$$

where, $v_{i,j}^{t}$ represents the speed of the *i*-th sparrow in the *j*-th dimension, $v_{i,j}^{t+1}$ represents the updated speed of the *i*-th sparrow in the *j*-th dimension, $x_{i,j}^{t}$ represents the position of the *i*-th sparrow in the *j*-th dimension, $x_{i,j}^{t+1}$ represents the updated position of the *i*-th sparrow in the *j*-th dimension, $x_{p,j}^{t}$ represents the position of the optimal explorer in the *j*-th dimension, $x_{g,j}^{t}$ represents the position of the global optimum in the *j*-th dimension, R_1 and R_2 respectively represent the uniform random numbers in (0, 1].

In addition, a danger warning mechanism is introduced. When there are predators around, the sparrows will change their positions to avoid being preyed upon. The position update equation for the danger warning is as follows:

$$x_{i,j}^{t+1} = \begin{cases} x_{best,j}^{t} + N(0,1) \cdot \left|x_{i,j}^{t} - x_{best,j}^{t}\right| & if\ f_i^t > f_g^t \\ x_{i,j}^{t} + K \cdot \left(\frac{\left|x_{i,j}^{t} - x_{worst,j}^{t}\right|}{f_i^t - f_w^t + \varepsilon}\right) & if\ f_i^t = f_g^t \end{cases} \tag{18}$$

where, $x_{i,j}^{t}$ represents the position of the *i*-th sparrow in the *j*-th dimension, $x_{best,j}^{t}$ represents the position of the best sparrow in the *j*-th dimension, $x_{worst,j}^{t}$ represents the position of the worst sparrow in the *j*-th dimension, f_i^t represents the fitness value of the i-th sparrow, f_g^t represents the global optimal fitness value, f_w^t represents the global worst fitness value, $N(0,1)$ represents a standard normal distribution random number, K represents a random number in $[-1,1]$, ε represents a small constant, used to avoid the denominator being zero.

Finally, repeat the above steps until the stopping condition is met, which is usually reaching the maximum number of iterations or reaching the preset target value.

Output the position and fitness of the best sparrow as the optimal solution or approximate optimal solution of the optimization problem.

3.2. Induction heating temperature control analysis

According to prior knowledge, the mathematical model of the CFRP induction heating system can be expressed as a first-order inertia system with a lag link, and its equation is as follows:

$$G(s) = \frac{K}{Ts+1} \cdot e^{-Ls} \tag{19}$$

where K represents the inertia gain, T represents the inertia time constant, and L represents the lag time.

This experiment is based on open-loop induction heating for data collection. The temperature value is collected every 0.5 seconds, and the total heating time is 2000 seconds. A genetic algorithm is used to identify and fit the parameters. The final transfer function equation for the system is as follows:

$$G(s) = \frac{195.78}{221.1s+1} \cdot e^{-11.82s} \tag{20}$$

In order to study the accuracy and anti-interference ability of SSA-PID control in the temperature control of CFRP induction heating, this paper uses MATLAB/Simulink as the simulation platform and establishes the control model of the induction heating CFRP temperature control system. In the same simulation environment, PID, the PSO-PID algorithm, and SSA-PID are compared and analyzed. The Simulink model is shown in **Figure 5**, where line 1 represents PID control and line 2 represents PSO-PID and SSA-PID, respectively.

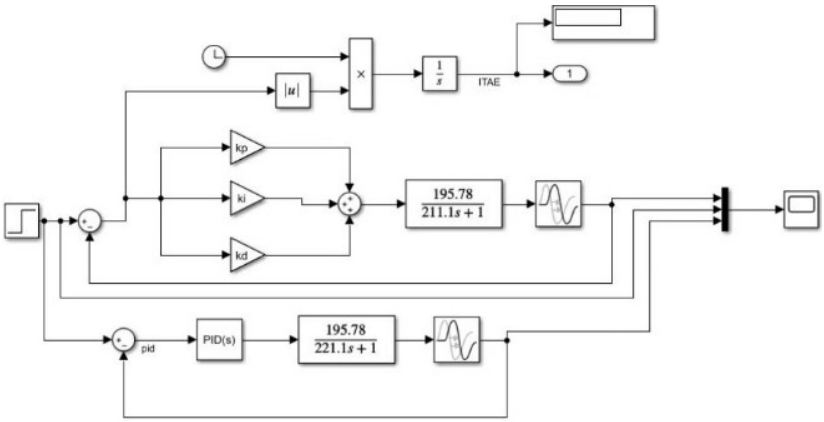

Figure 5. Simulation of induction heating temperature control simulink.

Figure 6 shows the fitness value and parameter change curve obtained by the simulation model of the PID temperature control method optimized by the sparrow search algorithm. It can be seen from the figure that with the increase in iteration times, the proportion, integral, and differential coefficients are gradually adjusted and finally stabilized, indicating that the sparrow search algorithm has good adaptability and anti-interference characteristics in the CFRP induction heating control process. In addition, the PID parameters will be automatically adjusted with the change in temperature conditions.

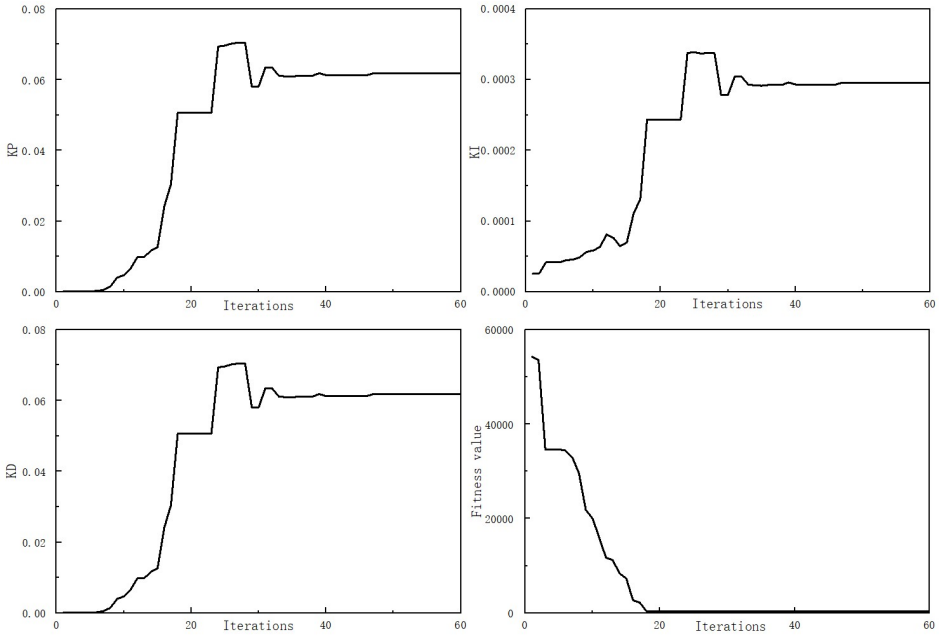

Figure 6. Change curve of proportional, integral, and differential coefficients.

As shown in **Figure 7**, the comparison of the three control algorithms for the CFRP induction heating system shows that all three control algorithms eventually achieved stable control. The traditional PID control system reached a steady state in 142.5 s, the PSO-PID control system reached a steady state in 99 s, and the SSA-PID control system reached a steady state in 91.5 s. Compared with the traditional PID control, the PSO-PID control system and the SSA-PID control system both have faster response speeds and smaller overshoots. By comparing the PSO-PID and SSA-PID control systems, it can be seen that the SSA-PID control system is superior to the PSO-PID control system, mainly manifested in the SSA-PID control system has a faster response speed and a smaller overshoot. Under the fact that the SSA-PID control method, the temperature rise time, overshoot, adjustment time, and steady-state error are minimized. This indicates that this control method has better dynamic performance than the traditional control method, effectively improving the material forming quality.

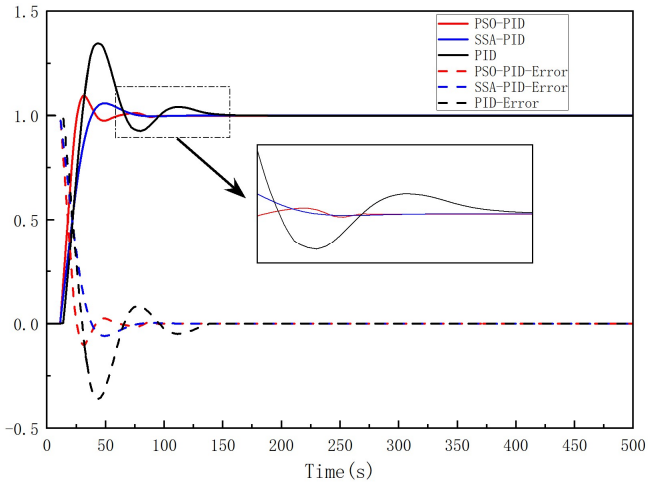

Figure 7. Adaptive response of three control methods.

4. Conclusion

In order to improve the temperature control accuracy and reduce the errors caused by the heating lag of carbon fiber cloth and the inherent delay of the temperature control system, this paper uses COMSOL as the platform, performs temperature field analysis and calculation on the induction heating CFRP temperature control system, collects the temperature output data from the initial state to the steady state of the induction heating system, and uses a genetic algorithm to identify the system mathematical model of the induction heating CFRP system. Matlab is used to simulate and verify the temperature control model, and the simulation results of the PID, PSO-PID, and SSA-PID algorithms are compared and analyzed. It is observed that the SSA-PID controller has good performance, obtaining the minimum overshoot, the shortest rise time, and the minimum adjustment time. Compared with the traditional PID control method, SSA-PID shows significantly improved stability and accuracy, which also indicates that the SSA-PID established in this study can more effectively adjust the heating curve in the CFRP heating process.

Author contributions: Conceptualization, NY and TF; methodology, NY; validation, NY and TF; formal analysis, NY; writing—original draft preparation, NY; writing—review and editing, NY; visualization, NY supervision, TF; project administration, TF; funding acquisition, TF. All authors have read and agreed to the published version of the manuscript.

Funding: This work was supported by the National Natural Science Foundation of China [grant number 52303031] and the Research Laboratory of Carbon Fiber Pressure Vessel Forming Technology [grant number KYPT202203Z].

Conflict of interest: The authors declare no conflict of interest.

References

1. Fink BK, McCullough RL, Gillespie JW. A local theory of heating in cross-ply carbon fiber thermoplastic composites by magnetic induction. Polymer Engineering & Science. 1992; 32(5): 357-369. doi: 10.1002/pen.760320509
2. Yarlagadda S, Kim HJ, Gillespie JW, et al. A Study on the Induction Heating of Conductive Fiber Reinforced Composites. Journal of Composite Materials. 2002; 36(4): 401-421. doi: 10.1177/0021998302036004171
3. Kim HJ, Yarlagadda S, Shevchenko NB, et al. Development of a Numerical Model to Predict In-Plane Heat Generation Patterns During Induction Processing of Carbon Fiber-Reinforced Prepreg Stacks. Journal of Composite Materials. 2003; 37(16): 1461-1483. doi: 10.1177/0021998303034460
4. Lundström F, Frogner K, Wiberg O, et al. Induction heating of carbon fiber composites: Investigation of electrical and thermal properties. Di Barba P, Dughiero F, Forzan M, Sieni E, eds. International Journal of Applied Electromagnetics and Mechanics. 2017; 53: S21-S30. doi: 10.3233/jae-162235
5. Ravari ARN, Taghirad HD. A novel hybrid Fuzzy-PID controller for tracking control of robot manipulators. 2008 IEEE International Conference on Robotics and Biomimetics. Published online February 2009. doi: 10.1109/robio.2009.4913244
6. Howell MN, Best MC. On-line PID tuning for engine idle-speed control using continuous action reinforcement learning automata. Control Engineering Practice. 2000; 8(2): 147-154. https://doi.org/10.1016/S0967-0661(99)00141-0
7. Meshram PM, Kanojiya RG. Tuning of PID controller using Ziegler-Nichols method for speed control of DC motor. In: IEEE-International Conference On Advances In Engineering, Science And Management (ICAESM -2012); 30-31 March 2012; 117-122.
8. Duan, H, Wang, D, Yu, X. Novel approach to nonlinear PID parameter optimization using ant colony optimization algorithm. Journal of Bionic Engineering. 2006; 3: 73-78. https://doi.org/10.1016/S1672-6529(06)60010-3

9. Varol HA, Bingul Z. A new PID tuning technique using ant algorithm. Proceedings of the 2004 American Control Conference. Published online 2004. doi: 10.23919/acc.2004.1383780
10. Boubertakh H, Tadjine M, Glorennec PY, et al. Tuning fuzzy PD and PI controllers using reinforcement learning. ISA Transactions. 2010; 49(4): 543-551. doi: 10.1016/j.isatra.2010.05.005
11. Aghaei VT, Onat A, Eksin I, et al. Fuzzy PID controller design using Q-learning algorithm with a manipulated reward function. 2015 European Control Conference (ECC). Published online July 2015. doi: 10.1109/ecc.2015.7330914
12. Wen X, Wang J. Fuzzy PID Controller Based on Improved Neural Network for Satellite Attitude. 2015 Fifth International Conference on Instrumentation and Measurement, Computer, Communication and Control (IMCCC). Published online September 2015. doi: 10.1109/imccc.2015.259
13. Soyguder S, Alli H. Fuzzy adaptive control for the actuators position control and modeling of an expert system. Expert Systems with Applications. 2010; 37(3): 2072-2080. doi: 10.1016/j.eswa.2009.06.071
14. Chang CJ, Chiang TH, Tai CC. A modified self-tuning fuzzy logic temperature controller for metal induction heating. Review of Scientific Instruments. 2020; 91(6). doi: 10.1063/5.0006019
15. Chowdhury JI, Thornhill D, Soulatiantork P, et al. Control of Supercritical Organic Rankine Cycle based Waste Heat Recovery System Using Conventional and Fuzzy Self-tuned PID Controllers. International Journal of Control, Automation and Systems. 2019; 17(11): 2969-2981. doi: 10.1007/s12555-018-0766-6
16. Wang Y, Cao F. Induction Heating Power Supply Temperature Control Based on a Novel Fuzzy Controller. 2008 International Conference on Computer and Electrical Engineering. Published online December 2008. doi: 10.1109/iccee.2008.64